CFD Letters

Journal homepage: www.akademiabaru.com/cfdl.html
ISSN: 2180-1363

Effects of Severity and Dominance of Viscous Force on Stenosis and Aneurysm During Pulsatile Blood Flow Using Computational Modelling

Open Access

Md. Abdul Karim Miah[1,*], Shorab Hossain[2], Sayedus Salehin[1]

[1] Department of Mechanical and Production Engineering, Islamic University of Technology (IUT), Board Bazar, Gazipur-1704, Dhaka, Bangladesh
[2] King Fahd University of Petroleum & Minerals, Dhahran, Saudi Arabia

ARTICLE INFO

Article history:
Received 20 June 2020
Received in revised form 19 August 2020
Accepted 24 August 2020
Available online 30 August 2020

Keywords:
Aneurism; stenosis; Womersley Number (W_0); wall shear stress

ABSTRACT

Cardiovascular diseases are the predominant cause of the death globally. It has become a challenge for the clinicians to understand the behavior of the stenoses and aneurysms at different stages of the growth. A numerical analysis based on a finite volume approach is employed for a 2-D axisymmetric, incompressible, laminar flow to simulate and compare the pulsatile blood flow in the models of arterial stenosis and aneurysm of the same sizes. Two key parameters, Radial velocity distribution and wall shear stress (WSS) distribution, have been considered for analyzing and comparing stenosis and aneurysm of same sizes of 30% and 50% severity. These parameters have been compared using unsteady blood flow of two frequencies: Womersley number (W0) of 7.75 and 10. In addition, the extent of the effect of Womersley number (W0) has been discussed. A flow input waveform is presented in terms of sinusoid. The results implicate that the Womersley number has a little effect on the flow field when the sizes were varied, which indicates the dominance of viscous force on the flow field of the models considered. It has been observed that the severity of the stenosis or aneurysm has significant effect on the flow field and wall shear stress. It has been concluded that, for a particular depth of stenosis and aneurysm, with the same flow inputs, WSS is significantly high in the stenosis compared to that in aneurysm indicating severe risk in stenosis.

1. Introduction

Blood flow through artery is indeed complex and investigation of its flow behavior is essential for its use in life science and medical technology. Since the hemodynamics hypotheses of atherosclerosis were first formulated several decades ago, flow imaging and computing have played an increasingly important role in advancing our understanding of how blood really flows in large arteries [1] prone to atherosclerosis [2]. Many experimental and CFD analysis have been carried out to investigate the

* *Corresponding author.*
E-mail address: akarim@iut-dhaka.edu (Md. Abdul Karim Miah)

https://doi.org/10.37934/cfdl.12.8.3554

flow disorder due to formation of aneurysm, in human beings leading to the failure of cardiovascular system [3-7].

Arterial stenosis is an abnormal narrowing of one of the arteries, as defined by the national institute of neurological disorders and stroke. Several studies related to hemodynamic characteristics of flow around a deformable stenosis were analyzed in various studies [8-10]. Aneurysm is an excessive localized enlargement of an artery caused by weakness in the artery wall**.** The presence of a stenosis or an aneurysm in an artery may significantly alter the flow field and consequently the flow rate, leading to severe pathological incidences. Stenosis increases the risk for ischaemic stroke as it reduces blood flow. The heart then needs to squeeze (contract) harder to pump blood, whereas the development of an aneurysm and its continuous dilation may lead to its rupture causing death or grave disability.

The main goal of blood flow simulation in vessels is to evaluate hemodynamic forces which artery wall experiences due to different factors e.g. the pulsatile blood flow, the fluid flow geometry and the blood rheology behavior (Quasi-Newtonian or non-Newtonian fluid). Besides, it is important to know if there is any observable correlation between flow pattern characteristics and abnormal biological events and arterial diseases.

It is proved that hemodynamic parameters play fundamental roles in regulating vascular biology and also in assessing of arterial diseases [11]. Most important hemodynamic parameters are -wall shear stress, arterial wall strain, particle residence time and recirculation zones. Formations of dysfunctions in vascular biology are results of irregular variation of these parameters.

Several numerical and experimental works have been carried out to observe the blood flow behaviors using aneurysm or/and stenosis models considering the flow as pulsatile using both 2D and 3D approach and also using rigid and flexible wall [12,13].

Ojha *et al.,* [14] experimentally investigated flow behavior through arterial stenosis. They used photochromic tracer method to find out the velocity profile of pulsatile flow choosing three axial locations in a flow channel by applying a 2.9 Hz sinusoidal flow to find out the flow patterns in vessels having different degrees of constriction. Türk *et al.,* [15] investigated the behavior of the bio fluid through symmetric stenosis of 40% and 60% constriction placed under magnetic source and found the flow to be affected by the presence of both stenosis and magnetic field. Mittal *et al.,* [16] studied pulsatile blood flow through modeled arterial stenosis with 50% semicircular constriction and showed that the flow downstream of the stenosis exhibited all the classic features of post-stenotic flow. Womersley number is widely used in transient fluid flow. Womersley number indicates how is the transient inertial effect compared to the viscous effects. Modarres *et al.,* [17] computed hemodynamic wall parameters at three Womersley numbers and it was found that the time-averaged reattachment point is maximum for the Newtonian model and minimum for the Power law model. Ikbal *et al.,* [18] also carried out investigation using a rheology of blood that is characterized by generalized Power law model. Hasan *et al.,* [19] studied the effect of pulsation, stenosis size, Reynolds Number and Womersley number for the laminar flow through a model arterial stenosis. Ali *et al.,* [20] presented a mathematical study for unsteady pulsatile flow of blood through a tapered stenotic artery. The constitutive equation for Sisko model [20] is used to illustrate the rheology of blood. The axial velocity of blood, resistance to flow, flow rate and wall shear are significantly influenced by blood rheology wall movement, presence of stenosis and degree of taperness of the artery. Ishikawa *et al.,* [21] numerically analyzed periodic blood flow through a stenosed tube. They concluded that non-Newtonian property reduces the strength of the vortex downstream of stenosis and has considerable influence on the flow. Kumar *et al.,* [22] carried out numerical analysis on nonlinear axisymmetric pulsatile blood flow. The result shows a significant effect of the presence of aneurysm on a number of parameters: wall shear, central axis velocity, pressure gradient, central axis and wall pressures. Miah *et al.,* [23] investigated blood flow behavior in few stenoses of same severity but of different lengths and concluded that smaller length stenosis shows high value of wall shear stress.

Husain *et al.,* [24] carried out investigation on pulsatile flow of blood through stenosis and aneurysm using four non-Newtonian models of blood. They finally quantified the effects of different models and came to the conclusion about which of the models was appropriate over a specified range of shear rates. Gopalakrishnan *et al.,* [25] also investigated pulsatile blood flow through aneurysm models. They conclude that aneurysm could be viewed as a 'wave-maker' and it accounts for the disturbances in the flow in the healthy segments of the artery.

Considerable amount of works has been done to observe the variation of different parameters in the blood flow in different modeled stenosis and also aneurysm. Stenosis and aneurysm of different shapes and sizes were studied [15,19,22-25,31-32]. Several works have been done on the combination of stenosis and aneurysm in the same arterial location [26-29]. However, to the best of author's knowledge, no studies have been attempted to compare the flow behavior for the same sized stenosis and aneurysm. In this numerical modeling, the blood flow behavior using the stenosis and aneurysm of the same size, or depth, has been studied to investigate the effects of laminar sinusoidal flow through the modeled artery.

2. Methodology

2.1 Mathematical Modelling

General continuity and Navier-Stokes equation for the fluid flow is reduced for axisymmetric flow of incompressible, Newtonian fluids. The general continuity equation for fluid flow

$$\frac{\partial \rho}{\partial t} + \Delta.(\rho \boldsymbol{u}) = 0$$

which for incompressible flow in two-dimensional cylindrical co-ordinate (r, Z) can be reduced to

$$\frac{1}{r}\frac{\partial (r\boldsymbol{u}_r)}{\partial z} + \frac{\partial (\boldsymbol{u}_z)}{\partial z} = 0$$

General form of Navier-Stokes equation (with no body force) in the vector form is

$$\rho\frac{\partial \boldsymbol{u}}{\partial t} + \rho\boldsymbol{u}.\nabla\boldsymbol{u} = -\nabla \mathrm{p} + \nabla^2\boldsymbol{u}$$

which for incompressible flow in two-dimensional cylindrical co-ordinate (r, Z) can be reduced to the following.

Momentum in r direction

$$\frac{\partial \boldsymbol{u}_r}{\partial t} + \boldsymbol{u}_r\frac{\partial \boldsymbol{u}_r}{\partial r} + \boldsymbol{u}_z\frac{\partial \boldsymbol{u}_r}{\partial z} = -\frac{1}{\rho}\frac{\partial p}{\partial r} + \frac{\mu}{\rho}[\frac{\partial}{\partial r}(\frac{1}{r}\frac{\partial (r\boldsymbol{u}_r)}{\partial r} + \frac{\partial^2 \boldsymbol{u}_r}{\partial z^2})]$$

Momentum in Z-direction

$$\frac{\partial \boldsymbol{u}_z}{\partial t} + \boldsymbol{u}_r \frac{\partial \boldsymbol{u}_z}{\partial r} + \boldsymbol{u}_z \frac{\partial \boldsymbol{u}_z}{\partial z} = -\frac{1}{\rho}\frac{\partial p}{\partial z} + \frac{\mu}{\rho}[\frac{1}{r}\frac{\partial}{\partial r}\left(r\frac{\partial(\boldsymbol{u}_z)}{\partial r} + \frac{\partial^2 \boldsymbol{u}_z}{\partial z^2}\right)]$$

Here, r = radial co-ordinate, z = axial co-ordinate locating at the axis of the symmetrical tube, $\mathbf{u}_r$ = total velocity in radial direction, $\mathbf{u}_z$ = total velocity in axial direction, p=pressure, ρ = density and μ = dynamic viscosity

2.2 Two-Dimensional Computational Models of Artery and Stenosis

The stenosis and aneurysm models, as shown in Figure 1, represents the geometry of the stenosis and aneurysm used in the simulations, where L=length at the end portion, D=diameter of the unaffected tube, $\boldsymbol{\delta}$ = depth of stenosis/aneurysm, Z'=Z/D (normalized distance from the center of the models.

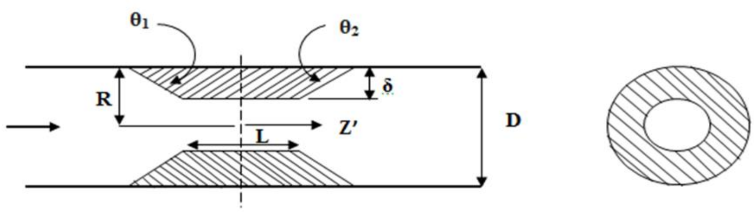

(a)

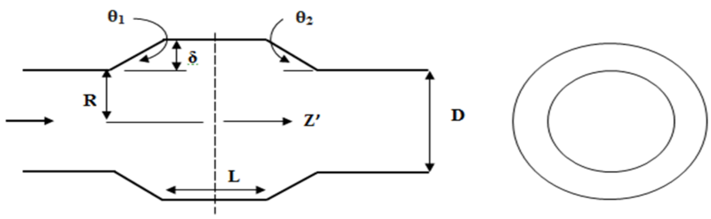

(b)

Fig. 1. Geometry of the (a) stenosis and (b) aneurysm used in the simulations, where L=length at the end portion, D=diameter of the unaffected tube, $\boldsymbol{\delta}$ = depth of stenosis/aneurysm, Z'=Z/D (normalized distance from the center of the models. on the right side is the cross-sectional view of models)

Stenosis severity has been defined as

$$\frac{depth\ of\ the\ stenosis}{unaffected\ tube\ diameter} = \frac{2\delta}{D} = \frac{\delta}{R}$$

Aneurysm severity has been defined as

$$\frac{depth\ of\ the\ aneurysm}{unaffected\ tube\ diameter} = \frac{2\delta}{D} = \frac{\delta}{R}$$

For the present numerical simulation in Figure 1, $\theta_1=45^0$, $\theta_2=45^0$ and L=2mm have been considered. And for the validation from Ojha *et al.,* [14], in Figure 1 (a), $\theta_1=30^0$, $\theta_2=45^0$ and L=1.5mm have been considered for the model. Stenosis and aneurysm models of 30% and 50% severity have been considered for the simulation as taken in [16-17,19,23,29-31].

2.3 Grid Independence Test of Stenosis and Aneurysm

Numerical results should be independent of the inlet and outlet lengths of the artery from the stenosis or aneurysm. To find the independent inlet and outlet lengths from the stenosis/aneurysm, several simulations were carried out. Finally, it was seen that 20D and 60D lengths were sufficient for the proximal and distal side of the aneurysm and stenosis respectively. To ensure the accuracy of the simulated results, several simulations were carried out with different mesh/gird shapes, several calculations were done with different number of elements. Finally, the chosen shape was the quadrilateral in 2D space as shown in Figure 2, and different optimized elements for different stenosis grids and aneurysm grids were chosen: 50592 for 30% stenosis, 50597 for 50% stenosis, 51648 for 30% aneurysm, and 52400 for 50% aneurysm. The computational results with quadrilateral shaped grid have been shown in the Table 1.

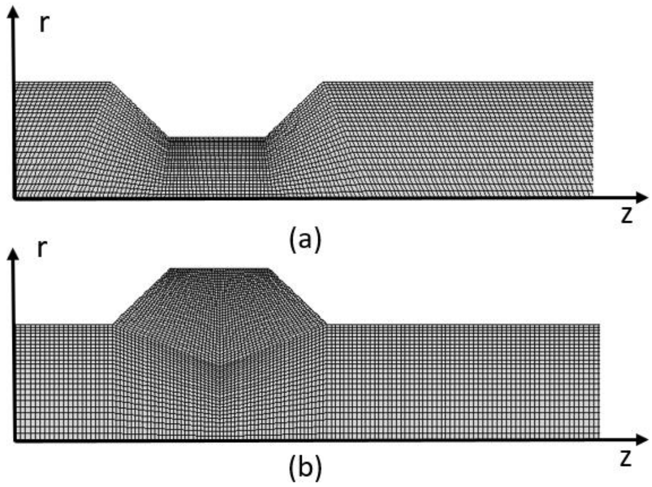

Fig. 2. Discretization of the computational domains of (a) stenosis and (b) aneurysm

Table 1
Grid Independency test for Re=575, Wo =7.75

Stenosis				Aneurysm			
30%		50%		30%		50%	
Elements number	Central axial velocity	Elements number	Central axial velocity	Elements number	Central axial velocity	Elements number	Central axial velocity
19035	0.9010	19206	1.480	19440	0.567	19986	0.5689
28458	0.9180	29244	1.520	32585	0.569	34264	0.5680
41778	0.9183	41826	1.521	42636	0.569	44426	0.5693
50592	0.9183	50976	1.521	51648	0.569	52400	0.5693
65035	0.9182	65632	1.521	66586	0.569	68564	0.5693

2.4 Boundary Conditions in the Present Computation
2.4.1 At inlet

At the inlet of the computational domain, 'velocity inlet' boundary condition is used. The same sinusoidal volume flow as Ojha *et al.,* [14] with a phase shift of 128^0 (123miliseconds) [19] in Figure 3 (a). The velocity is found out by dividing the volume flow rate with the area.

$$Q= 4.3+2.6 \sin \left(\frac{2\pi t}{T}\right)$$

$$v_{inlet} = \frac{Q}{Area}$$

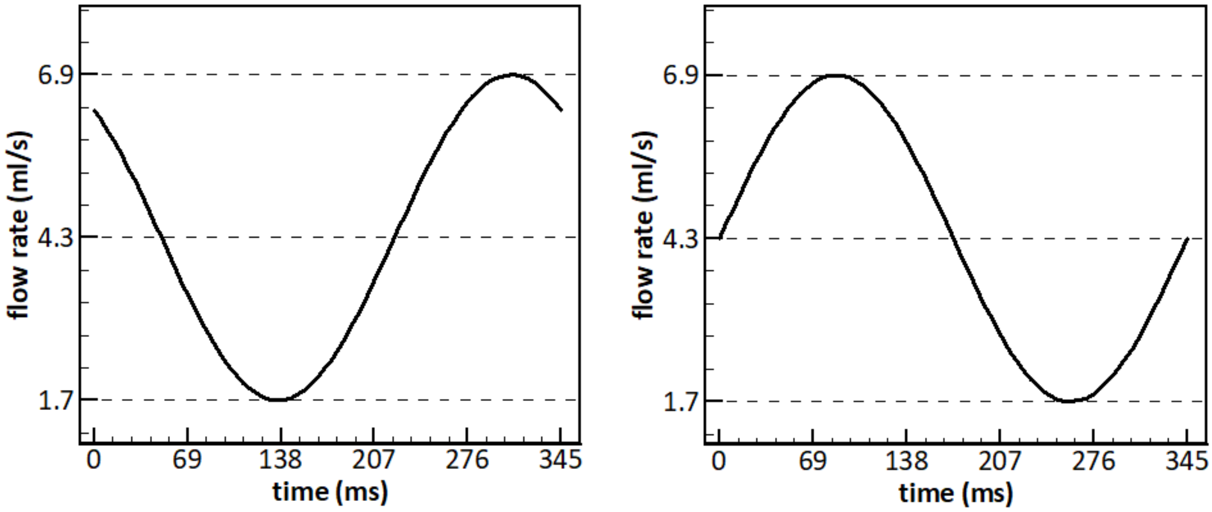

(a) (b)

Fig. 3. Volumetric flow at the inlet of the artery in (a) Ojha *et al.,* [14], and (b) present simulation

2.4.2 At outlet

At the outlet, the flow is considered fully developed. Zero normal gradient for all flow variables except pressure is considered. 'Outflow' boundary condition is used which satisfies the following equation

$$\frac{\partial \boldsymbol{u}_r}{\partial z} = \frac{\partial \boldsymbol{u}_z}{\partial z} = 0.$$

2.4.3 At centreline

In the computational domain, x axis has been considered as the axial symmetry condition.

2.4.4 At wall

No slip boundary with no flow ($u_z = u_r = 0$) is assumed at the wall section of the computational domain.

2.5 Validation of CFD code

To prove the acceptance of the numerical result for unsteady pulsatile laminar flow in this study, the results have been validated with experimental works from Ojha *et al.,* [14]. Time dependent centerline velocity distribution at different distal positions of the stenosis: Z' = 1, 2.5, 4.3 where Z' is taken as the normalized distance from the center of the stenosis and it is expressed as Z' =Z/D, where, D is the diameter and Z is the axial distance of the point from the middle point of the stenosis in axis line. The pulsatile flow has a time averaged flow of 4.3 ml/s with a sinusoidal flow of 2.9 Hz frequency having amplitude of 2.6 ml/s. 2.9 Hz frequency is equivalent to 345 ms of time period. The fluid density of 0.755 g/cm^3 and viscosity of 1.43 cP have been used which corresponds to the property of Deoderized Kerosen (shell-shol 715) at temperature of 20 ^{0}C. For the Newtonian assumption of the blood, the flow characteristic of the fluid (Kerosene) will be similar: for the same dimensionless number, Reynolds number. The Reynolds number considers the constriction free inner diameter of the artery, time-averaged mean velocity and constant viscosity for Newtonian behavior. Reynolds number is expressed as Re =VD/γ. The pulse applied at the inlet of the artery indicates a certain Womersley number. Womersley number indicates how is the transient inertial effect compared to the viscous effects and this number does not affect the Reynolds number. Here Womersley number is 7.75. The applied pulse corresponds to the mean Reynolds Number of 575 with a highest and lowest number of 930 and 230 respectively as shown in Figure 3 (a).

Before comparing velocity distribution at different distal points of the stenosis, centerline time varying/time dependent velocity is compared at the inlet of the stenosis, in Figure 4. It can be seen that velocities have a minor difference as smooth data has been used in simulation to approximate the experimental data. This little difference in the velocity causes discrepancy in the experimental and simulated results.

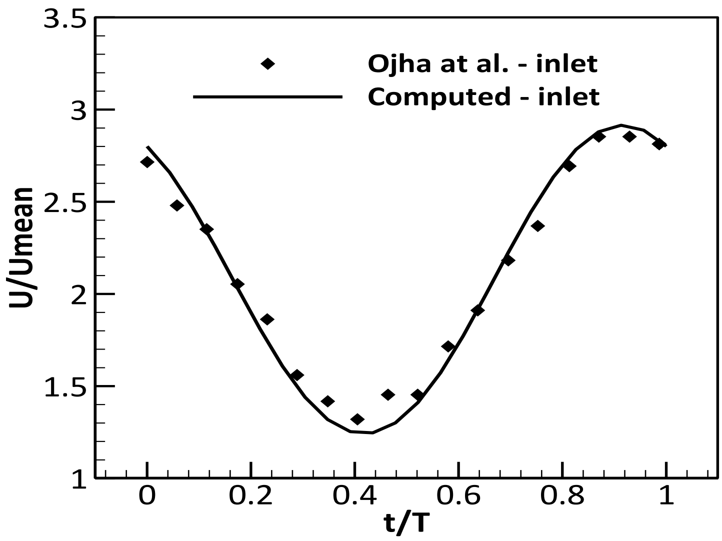

Fig. 4. Inlet centerline velocity profile

The experimental time varying velocity at different distal points has been compared with the results obtained from the simulation. There is a negligible error at the end of the period and the numerical calculation is acceptable.

3. Results

Fluctuating flow, with its effects, through the modeled arterial stenosis and arterial aneurysm will be discussed in detail here. Predominantly, the presence of arterial stenosis and arterial aneurysm of the same strength will be presented and compared to find the relatively dangerous one. To do so, radial velocity distribution at different arterial locations and wall shear stress have been considered as the parameters. In each section, the effects are presented for two flow frequencies: Wo=7.75, Wo=10. In total, two different sizes of both stenosis and aneurysm are shown: severity of 30% and severity of 50%. The model of the stenosis is the same as that of Ojha *et al.,* [14] with slight modification. The upstream angle of the stenosis has an angle of 45^0 and Length of the end portion is 2mm. The flow sinusoid is similar to that of Ojha *et al.,* [14] with a slight difference in the flow beginning. The present flow has a mean flow of 4.3 ml/s and amplitude of 2.6 ml/s as shown in Figure 5 and the flow began at angle of 0^0 whereas, in the model of Ojha *et al.,* [14], the flow started at 123^0.

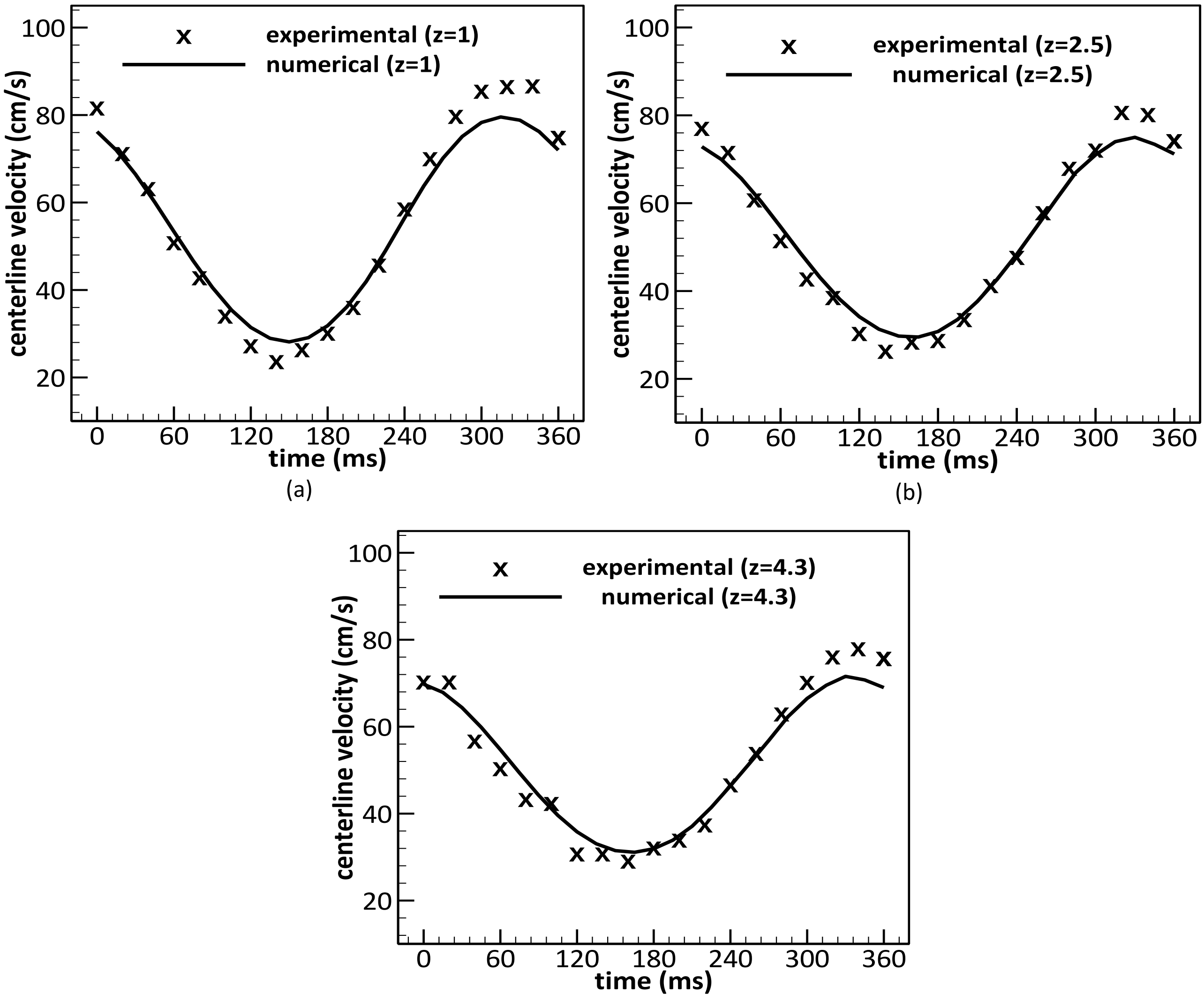

Fig. 5. Centerline axial velocity at (a) Z'=1, (b) Z'=2.5, and (c) Z'=4.3

3.1 Radial Velocity Distribution in Stenosis and Aneurysm

For analyzing the flow in stenosis and aneurysm, four key times- t/T=0, t/T=0.25 (maximum flow), t/T=0.50 and t/T=0.75 (minimum flow) have been considered. And, three key points – inlet, throat and outlet- have been considered for data presentation.

3.1.1 Radial velocity distribution in 30% stenosis and 30% aneurysm at Wo=7.75 and 10

In Figure 6, for the stenosis and aneurysm strength of 30%, the flow disturbances created in different cross sections of the stenosis and aneurysm are presented for Wo=7.75. The axial velocity profiles at Inlet section, as shown in Figure 6 (I), are different from the usual parabolic velocity profile. Though it is at the inlet section of the stenosis and the aneurysm, the profile/flow is affected as the flow is about to contract in stenosis and expand in the aneurysm at smaller and higher flow areas respectively. In both of the stenosis and aneurysm, at the beginning of the pulsatile flow, at t/T=0, the centerline velocity is slightly higher, about 2.1 times and 1.75 times of the steady flow/mean velocity for stenosis and aneurysm respectively. At t/T=0.25, when the flow is maximum, the centerline velocities are 3.18 times and 2.6 times of the mean velocity respectively. At t/T=0.50, the centerline velocities are 2.35 times and 2.1 times of the mean flow for stenosis and aneurysm respectively. The velocity is always lower in the region close to the wall for both the stenosis and aneurysm and this reduction of velocity is higher in stenosis compared to aneurysm. At inlet, the flow is slightly restricted because of the upstream stenosis but, for the aneurysm, no such restriction is there as the flow is going to be expanded in the upstream aneurysm. At t/T=0.75 for the minimum flow, the centerline velocities are 1.22 times and 1.2 times of the mean velocity. In every key point, closer to the centerline, the velocities in the stenosis are higher with respect to that of the aneurysm. It's because, for stenosis the flow is about to be narrowed in the stenosis at lower area increasing the velocity and for the aneurysm the flow is about to expand in the aneurysm at higher flow area reducing the velocity.

In Figure 6 (II), it shows the velocity distribution at the throat of the stenosis and aneurysm at different time steps. In this region, in the stenosis, the fluid accelerates and velocity reaches its maximum values, whereas, in the aneurysm, the fluid decelerates, because of the high flow areas, to the minimum values. Velocity profile for the stenosis becomes flattened indicating very high values compared to the steady velocity distribution. Flattened velocity distribution of the stenosis results in the thinning of the boundary layer. But for the aneurysm, the deflated velocity distribution results in the widening of the boundary layer. In the stenosis and aneurysm, at the beginning of the pulsatile flow, at t/T=0, the centerline velocities are 2.75 times and 1.65 times of the steady flow/mean velocity for stenosis and aneurysm respectively. At t/T=0.25 for the maximum flow, the centerline velocities are 4.2 times and 2.5 times of the mean velocity respectively. At t/T=0.50, the centerline velocities are 2.9 times and 2.05 times of the mean flow for stenosis and aneurysm respectively. At t/T=.75 for the minimum flow, the centerline velocities are 1.38 times and 1.15 times of the mean velocity. In every key point, the velocities in the stenosis are much higher with respect to that of the aneurysm.

In Figure 6 (III), it shows the velocity distribution at Outlet of the stenosis and aneurysm at different time steps. At the outlet of the stenosis, because of the abrupt rise of the area, the flow greatly slows down developing a possible boundary layer separation near the wall. But, the velocity towards the centerline increases as the flow is concentrated towards the central region. The velocity distribution for all the key times shows a region where flow becomes close to zero. This region spans 30% of the radius of the artery and after this region flattened velocity profile is seen. But the cases are completely different for the aneurysm, showing the velocity profiles almost the same as the inlet section of the aneurysm. In the aneurysm, the velocity distribution at the outlet did not have any considerable change from the velocity distribution at the inlet. And finally, closer to the centerline, the velocities are much higher in stenosis than in aneurysm.

In Figure 7, for the stenosis and aneurysm strength of 30%, with a flow having the Wo=10, the flow disturbances created in different cross sections of the stenosis and aneurysm have been shown. The velocity profiles observed at different sections are almost the same as that observed in Figure 6 with a slight variation of the values at different points. Finally, it can be concluded that the flow parameters for Wo=7.75 and Wo=10 are almost the same.

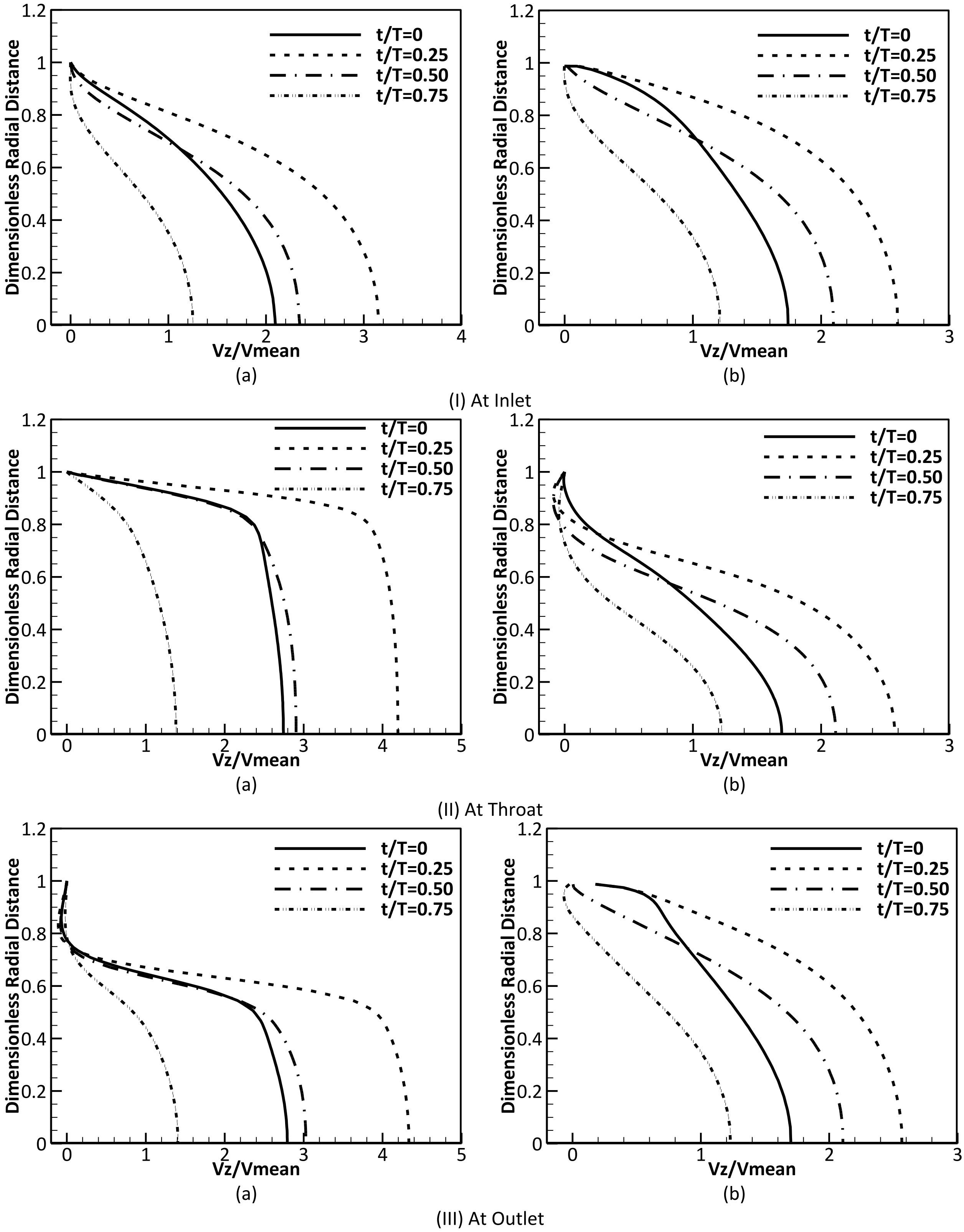

Fig. 6. Instantaneous radial velocity distribution at four key flow times at (I)Inlet, (II)Throat, and (III) Outlet of the (a) stenosis and (b) aneurysm at Wo=7.75

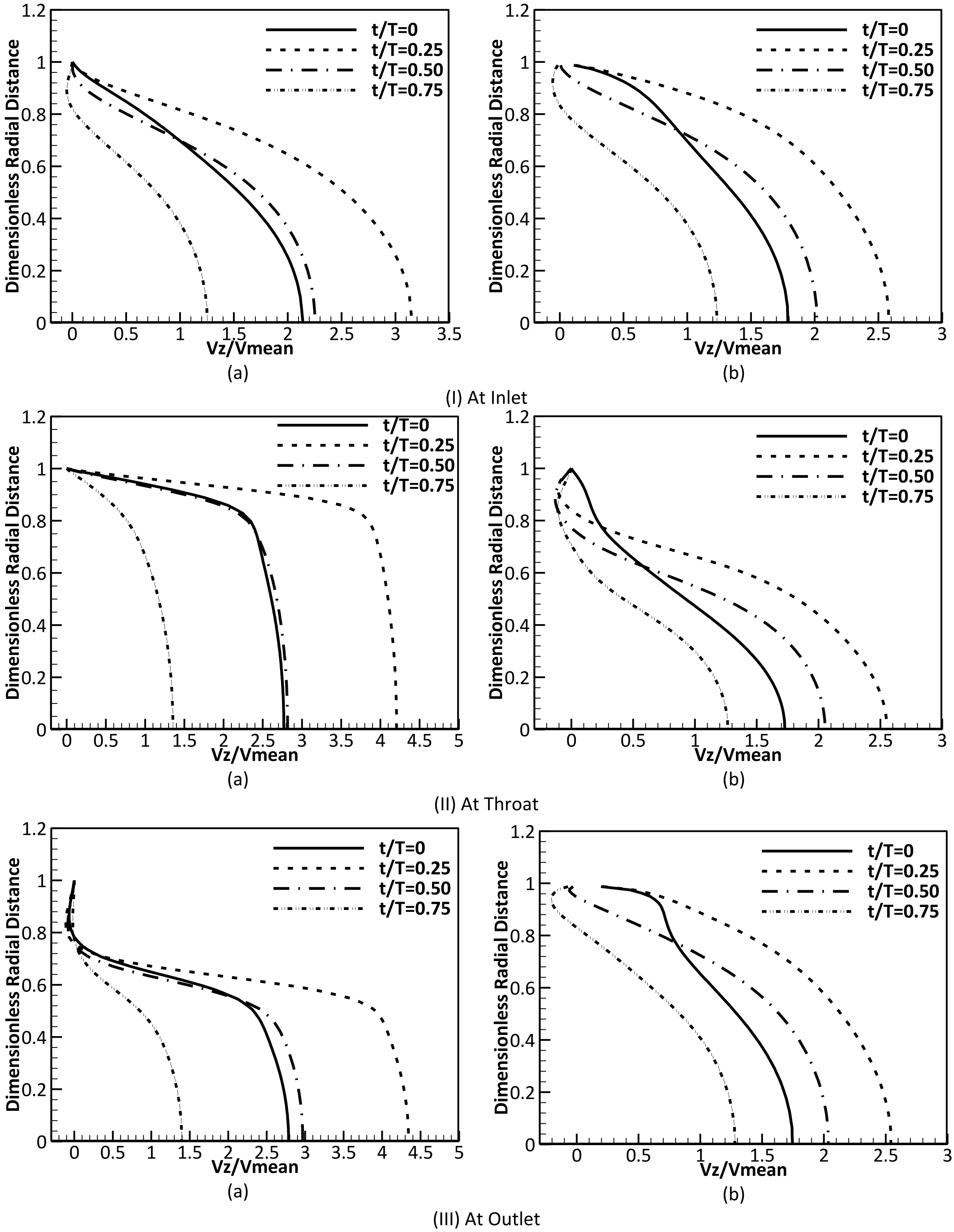

Fig. 7. Instantaneous radial velocity distribution at four key flow times at (I) Inlet, (II)Throat, and (III) Outlet of the (a) stenosis and (b) aneurysm at Wo=10

Penerbit
Akademia Baru

3.1.2 Radial velocity distribution in 50% stenosis and 50% aneurysm at Wo=7.75 and 10

In Figure 8 and Figure 9, for both the stenosis and aneurysm strength of 50%, with a flow having the Wo=7.75 and 10, the flow disturbances created in different key points have been shown.

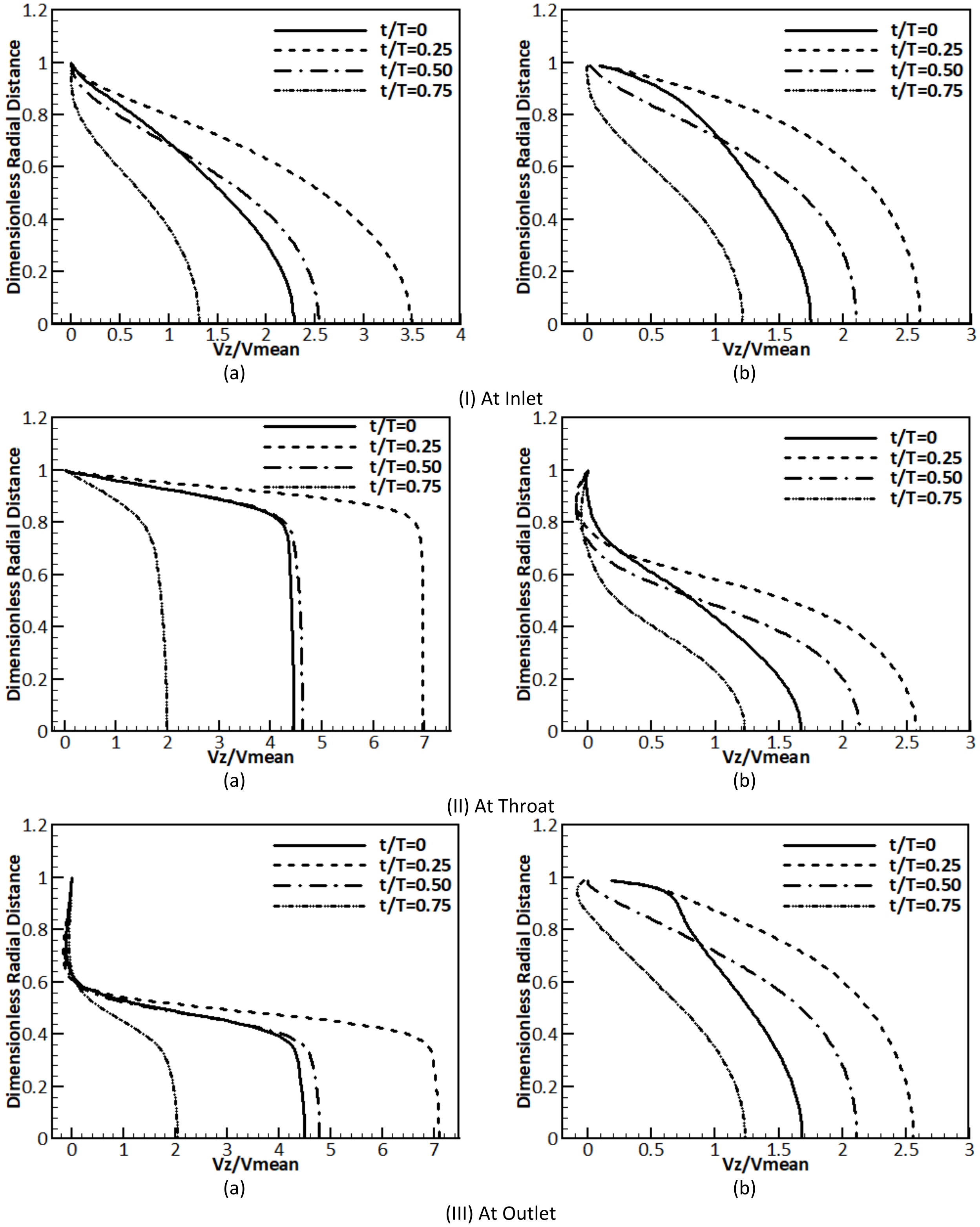

Fig. 8. Instantaneous radial velocity distribution at four key flow times at (I) Inlet, (II) Throat, and (III) Outlet of the (a) stenosis and (b) aneurysm at Wo=7.75

It has been observed that the radial velocity distributions are almost same as that in stenosis and aneurysm strength of 30% with a slight variation of the velocity values at different points.

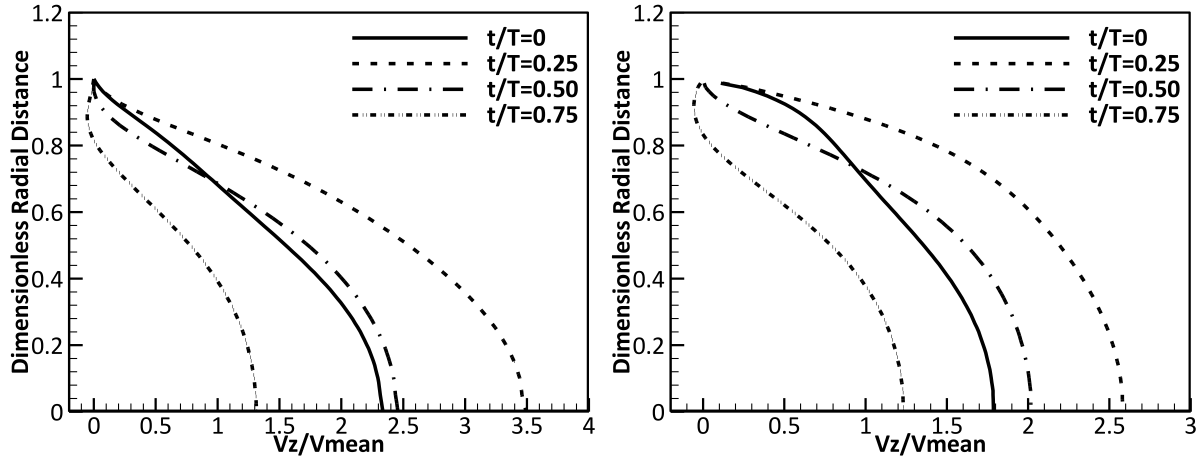

(a) (b)

(I) At Inlet

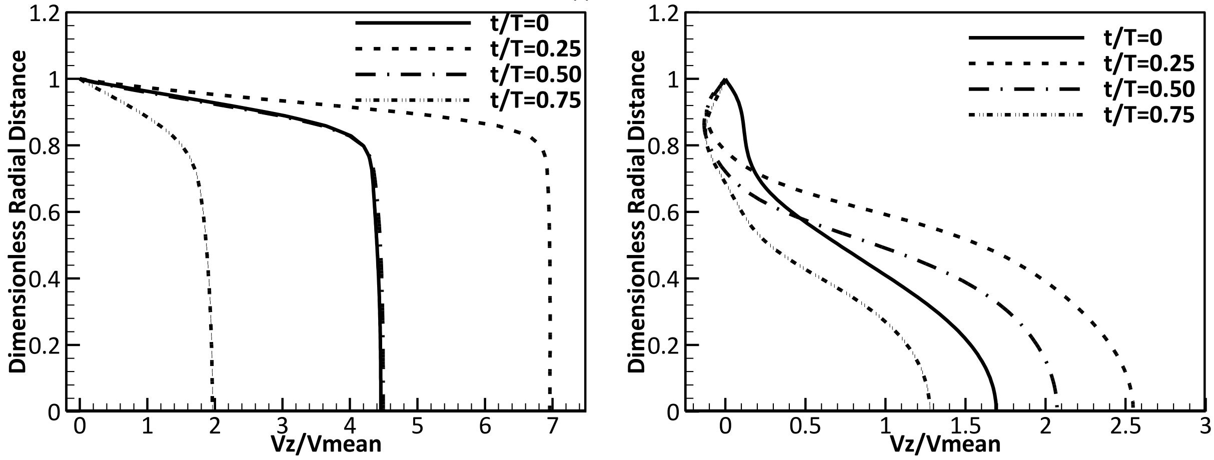

(a) (b)

(II) At Throat

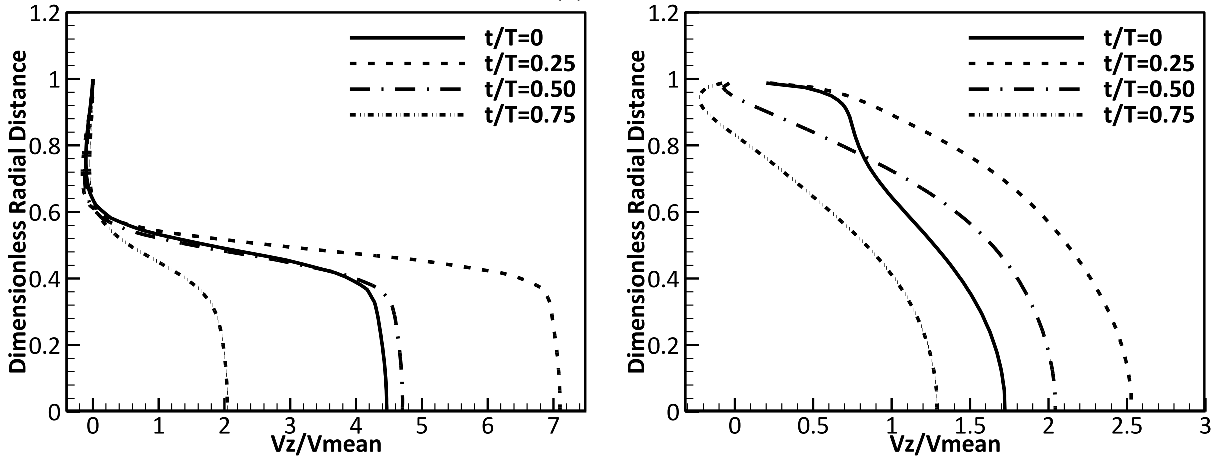

(a) (b)

(III) At Outlet

Fig. 9. Instantaneous radial velocity distribution at four key flow times at (I) Inlet, (II)Throat, and (III) Outlet of the (a) stenosis and (b) aneurysm at Wo=10

Finally, it can be concluded that change in Womersley number didn't make any significant change in the flow.

3.2 Wall Shear Stress (WSS) Distribution in Stenosis and Aneurysm

Wall shear stress is the determining hemodynamic parameter which will indicate the extent of risk of the patients. Wall shear stress at different key points at different key times will be discussed here for both stenosis and aneurysm for two flow frequencies.

3.2.1 WSS comparison between 30% stenosis and 30% aneurysm at Wo=7.75 and 10

Dimensionless axial distance is defined as the ratio of z (axial distance) and D (diameter), where z/D=0 indicates the mid position of the stenosis and aneurysm. Negative values indicate the locations at the left side or upstream side of the stenosis/aneurysm and positive values indicate the downstream side of the stenosis/aneurysm.

Here, in the Figure 10, for the 30% stenosis/aneurysm with a flow having Wo=7.75, the wall shear stress distributions along the axial direction in the wall for different key times are presented. It is observed that, for the stenosis, the WSS is highest at the inlet sections of the stenosis as the flow is hitting directly to the inlet side of the stenosis causing the abrupt increase of WSS, slightly higher throughout the stenosis area and finally drops down after the outlet sections. But for the aneurysm, the WSS behavior is different from that of stenosis. Here, the maximum WSS is found at the outlet sections of the aneurysm as the flow expanding form the inlet sides hits the outlet side creating high WSS. For the times when the fluid accelerates, the WSS maintains a bit higher value throughout the axial length and finally abruptly reduces and becomes minimum inside the aneurysm as flow is relaxed because of the aneurysmal expansion. At t/T=0, maximum WSS for stenosis and aneurysm are 18 and 2.4 respectively. At t/T=0.25, when the flow quickly accelerates, the maximum WSS for stenosis and aneurysm becomes 35 and 2.6 respectively. At t/T=0.50, the maximum WSS for stenosis and aneurysm becomes 15 and 0.5 respectively. At t/T=0.75, maximum WSS for stenosis and aneurysm are 3.0 and 0.2 respectively. Out of all times the maximum WSS is found when the flow accelerates at t/T=0.25. In all the cases, the maximum WSS developed in the stenosis is much higher than that developed in aneurysm.

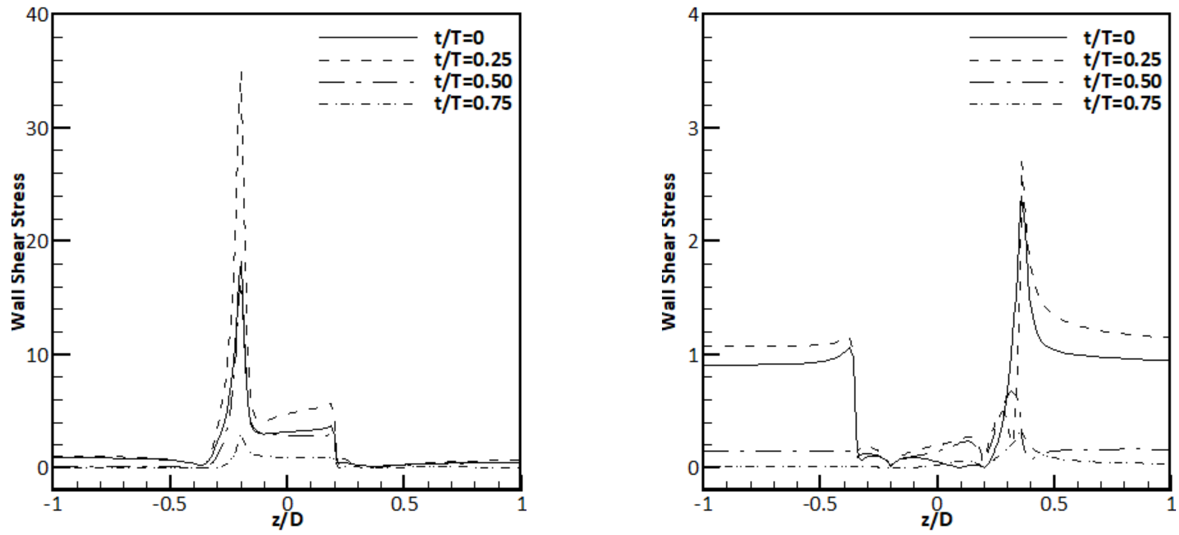

(a) (b)

Fig. 10. WSS distribution at four key flow time for (a)stenosis and (b) aneurysm at Wo=7.75

In Figure 11, for the 30% stenosis/aneurysm with a flow having Wo=10, the Wall Shear Stress distributions along the axial direction in the wall for different times are presented. It is clearly observed that the WSS distribution along the walls remains almost the same as that found for Wo=7.75 shown in Figure 10 indicating that the change in Womersley number didn't have any significant effect in wall shear stress distribution.

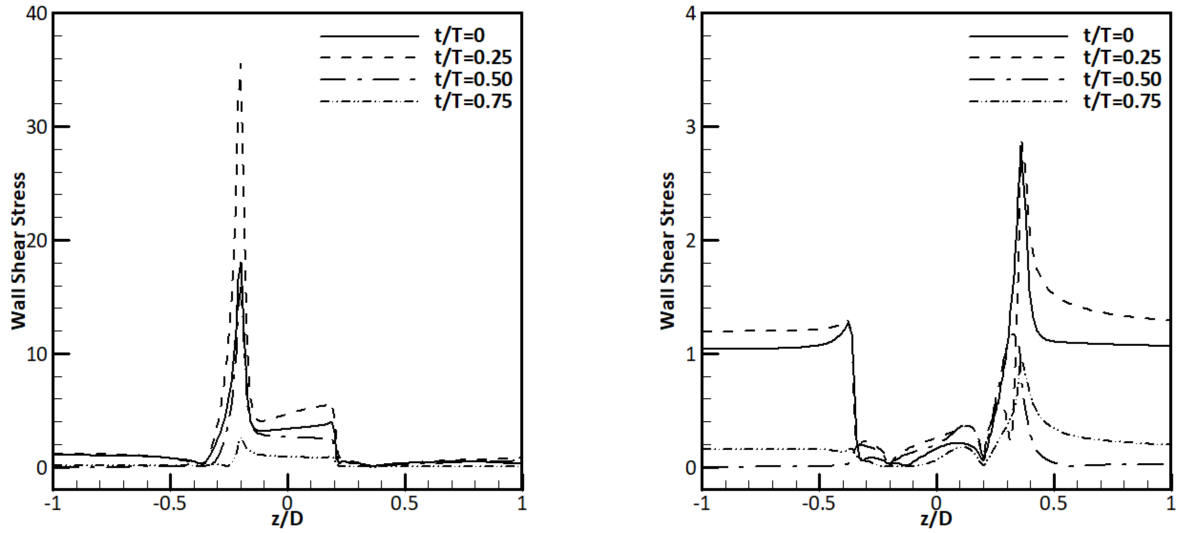

(a) (b)

Fig. 11. WSS distribution at four key flow time for (a)stenosis and (b) aneurysm at Wo=10

3.2.2 WSS comparison between 50% stenosis and 50% aneurysm at Wo=7.75 and 10

In Figure 12, for the 50% stenosis/aneurysm with a flow having Wo=7.75, the Wall Shear Stress distributions along the axial direction in the wall for different times are presented. The shear stress distribution pattern in Figure 12 and Figure 13 is same as that in Figure 10 and Figure 11, respectively, with the change in values of the Shear Stress.

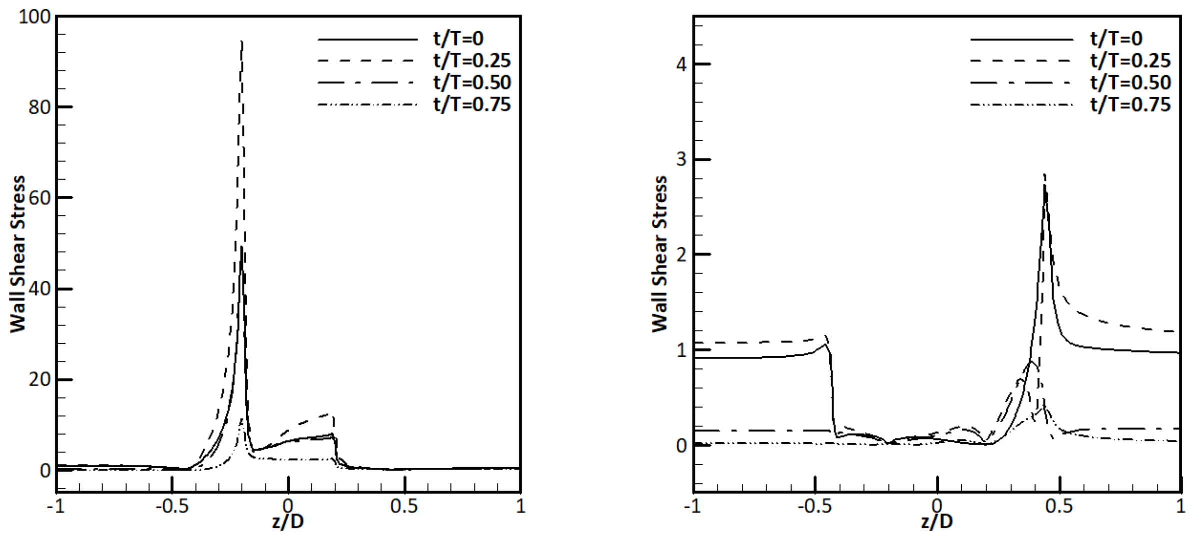

(a) (b)

Fig. 12. WSS distribution at four key flow time for (a)stenosis and (b) aneurysm for Wo=7.75

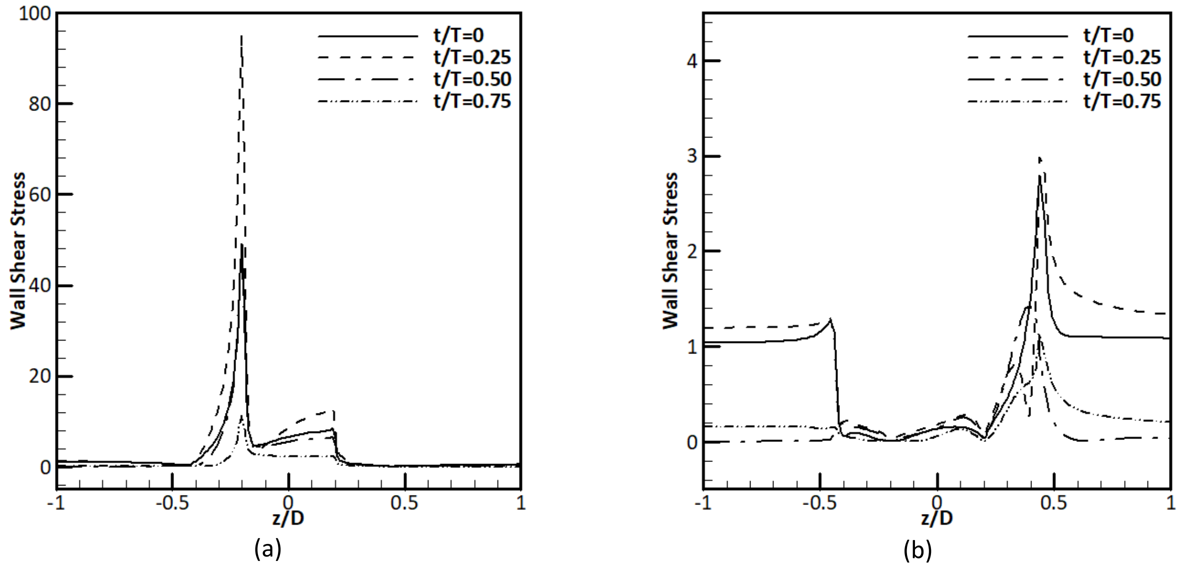

Fig. 13. WSS distribution at four key flow time for (a)stenosis and (b) aneurysm for Wo=10

3.3 Effect of Womersley Number

To evaluate the effects of Womersley number, the details of the velocity distribution and the change of the WSS for two different Womersley numbers were taken having the same Reynolds number. Effects were observed for different depths of stenosis and aneurysm. The Womersley numbers taken were 7.75 and 10 for a constant mean Reynolds number of 575 with a highest and lowest number of 930 and 230.

Womersley number is found to have a little effect in the velocity distribution both in the case of the stenosis and aneurysm for the particular models of stenosis and aneurysm used. The velocity magnitudes are not affected significantly for this change of the Womersley number from 7.75 to 10.

Because of the slight effect of Womersley number, indicating the dominance of viscous force, on the velocity distribution, it has also the same little effect on the WSS found both in the aneurysm and stenosis. Both 30% and 50% stenosis and aneurysm were observed and they have shown almost same type of effect. Womersley number is the physical interpretation of the effect of the unsteadiness to the viscous effect of the flow. Dynamic nature of the flow is greatly dependent on the flow frequency of the flow. For the two frequencies of time periods 345 milliseconds and 200 milliseconds it has been observed that viscous force is dominant in the flow of the chosen models of stenosis and aneurysm.

3.4 Effect of Size/Severity of Stenosis and Aneurysm

It can be said with certainty that size or the severity has great effect on the flow field of the constricted tubes of stenosis and less effect on aneurysm for the models considered. For investigating the effect of stenosis size/aneurysm size, different stenosis and aneurysm models with two different sizes have been studied. In the Inlet section, at t/T=.25 when the flow is accelerating, for the constant flow frequency, the centerline velocities of the stenosis and aneurysm are 3.18 and 2.6 times of the mean velocity for the 30% severity. Whereas, for 50% severity, centerline velocities are 3.5 times and 2.6 times of the mean velocities showing a large variation in the stenosis and insignificant variation of velocities in the aneurysm for the given models of stenosis and aneurysm. In the Throat, at t/T=.25 when the flow is accelerating, for the constant flow frequency, the centerline velocities of the stenosis and aneurysm are 4.2 and 2.5 times of the mean velocity for the 30% severity. Whereas, for

50% severity, centerline velocities are 6.95 times and 2.42 times of the mean velocities showing a large variation in the stenosis and small variation of velocities in the aneurysm for the given models of stenosis and aneurysm. When the depth of the stenosis is increased the flow area for the stenosis decreases and as such the velocity will increase but with the increase of the severity of the aneurysm the flow area increases. Though the flow is dependent on the total flow pattern inside the aneurysmal sac, the velocity is likely to decrease because of the increase of area.

As the size/severity has great effect on the velocity distribution of the stenosis and aneurysm, it will have great influence on the WSS distribution on the walls of the stenosis and aneurysm. WSS developed is maximum when the flow is accelerating that is at t/T=0.25. Maximum shear stresses developed in stenosis and aneurysms for the severity of 30% are 35 and 2.5 respectively. Whereas for 50% severity, the WSS becomes 95 and 3.0 respectively indicating 170% and 20% increase for stenosis and aneurysm respectively. They are measured for the same flow frequency.

In the aneurysm, with the increase of severity, the radial velocity at the throat has decreased but the WSS has increased. In the throat of aneurysm, the flow velocity has decreased as the area has increased. But, inside the sac/throat of aneurysm turbulence has increased with the increase of area. This turbulence causes the rise in the WSS.

For the particular models chosen for stenosis and aneurysm, it has been observed that the size/severity has great effect on the flow field and WSS. And the effects are much greater in stenosis than in aneurysm.

4. Conclusion

In the present study, a numerical simulation has been presented to investigate the effects of laminar sinusoidal flow through the modeled arterial stenosis and aneurysm. For both the models, the trapezoidal profile with an angle of 45^0 has been used to observe the effects on them. The models were axisymmetric. Sizes were varied from 30% severity to 50% severity. Inlet flow given was the sinusoidal pulsating with a mean Reynolds Number of 575 having maximum of 930 and a minimum value of 240. Womersley numbers of 7.75 and 10 with a time periods of 345 milliseconds and 200 milliseconds respectively were used to see the effect of the change of the flow pulsation. Radial velocity distribution and wall shear stress distribution have been observed to see the effects of change of Womersley number and sizes of the stenosis and aneurysm. From the numerical simulation, the following conclusions can be drawn

i. Variation of Womersley number is found to have a little effect in the velocity distribution both in the case of the stenosis and aneurysm for the particular models of stenosis and aneurysm used. This implies that the viscous force is dominant on the flow.
ii. As Viscous force is dominant on the flow, Womersley number has little effect on the WSS found both in the aneurysm and stenosis. Both 30% and 50% stenosis and aneurysm were observed and they have shown almost same type of effect.
iii. It can be stated with certainty that size or the severity of the stenosis has great effect on the flow field of stenosis while the severity shows a little effect for aneurysm for the particular models considered. In the Throat, at t/T=.25 when the flow is accelerating, for the constant flow frequency, the centerline velocity of the stenosis for 50% severity is 1.65 times of that of 30% severity. Whereas, the centerline velocity of the aneurysm for 50% severity is .97 times of that of 30% severity.
iv. As the size/severity has great effect on the velocity distribution of the stenosis, it will have great influence on the WSS distribution on the walls of the stenosis. WSS developed is maximum when the flow is accelerating that is at t/T=0.25. Maximum shear stresses

developed in stenosis and aneurysm of 50% shows 170% and 20% increase than that of 30% stenosis respectively.

v. For a particular depth of stenosis and aneurysm, with the same flow inputs, WSS is significantly high in the stenosis compared to that in aneurysm indicating very high risk in stenosis.
vi. It has been observed that, for the stenosis, the WSS is highest at the inlet sections of the stenosis as the flow is hitting directly to the inlet side of the stenosis causing the abrupt increase of WSS. But for the aneurysm, the WSS behavior is different from that of stenosis. Here, the maximum WSS is found at the outlet sections of the aneurysm as the flow expanding form the inlet sides hits the outlet side creating high WSS.

Acknowledgement
This research was not funded by any grant.

References

[1] Melicher, Valdemar, and V. Gajdošík. "A numerical solution of a one-dimensional blood flow model—moving grid approach." *Journal of Computational and Applied Mathematics* 215, no. 2 (2008): 512-520. https://doi.org/10.1016/j.cam.2006.03.065
[2] Berger, S. A., and Liang-Der Jou. "Flows in stenotic vessels." *Annual review of fluid mechanics* 32, no. 1 (2000): 347-382. https://doi.org/10.1146/annurev.fluid.32.1.347
[3] Reorowicz, Piotr, Damian Obidowski, Przemyslaw Klosinski, Wojciech Szubert, Ludomir Stefanczyk, and Krzysztof Jozwik. "Numerical simulations of the blood flow in the patient-specific arterial cerebral circle region." *Journal of biomechanics* 47, no. 7 (2014): 1642-1651. https://doi.org/10.1016/j.jbiomech.2014.02.039
[4] Khalafvand, Seyed Saeid, Eddie Yin-Kwee Ng, Liang Zhong, and Tin-Kan Hung. "Three-dimensional diastolic blood flow in the left ventricle." *Journal of biomechanics* 50 (2017): 71-76. https://doi.org/10.1016/j.jbiomech.2016.11.032
[5] Deplano, Valérie, Yannick Knapp, Lucie Bailly, and Eric Bertrand. "Flow of a blood analogue fluid in a compliant abdominal aortic aneurysm model: Experimental modelling." *Journal of biomechanics* 47, no. 6 (2014): 1262-1269. https://doi.org/10.1016/j.jbiomech.2014.02.026
[6] Imai, Yohsuke, Toshihiro Omori, Yuji Shimogonya, Takami Yamaguchi, and Takuji Ishikawa. "Numerical methods for simulating blood flow at macro, micro, and multi scales." *Journal of biomechanics* 49, no. 11 (2016): 2221-2228. https://doi.org/10.1016/j.jbiomech.2015.11.047
[7] Blanco, P. J., L. O. Müller, S. M. Watanabe, and R. A. Feijóo. "Computational modeling of blood flow steal phenomena caused by subclavian stenoses." *Journal of Biomechanics* 49, no. 9 (2016): 1593-1600. https://doi.org/10.1016/j.jbiomech.2016.03.044
[8] Choi, Woorak, Sung Ho Park, Hyung Kyu Huh, and Sang Joon Lee. "Hemodynamic characteristics of flow around a deformable stenosis." *Journal of Biomechanics* 61 (2017): 216-223. https://doi.org/10.1016/j.jbiomech.2017.07.033
[9] Pagiatakis, Catherine, Jean-Claude Tardif, Philippe L. L'Allier, and Rosaire Mongrain. "A numerical investigation of the functionality of coronary bifurcation lesions with respect to lesion configuration and stenosis severity." *Journal of biomechanics* 48, no. 12 (2015): 3103-3111. https://doi.org/10.1016/j.jbiomech.2015.07.018
[10] Sankaran, Sethuraman, Hyun Jin Kim, Gilwoo Choi, and Charles A. Taylor. "Uncertainty quantification in coronary blood flow simulations: impact of geometry, boundary conditions and blood viscosity." *Journal of biomechanics* 49, no. 12 (2016): 2540-2547. https://doi.org/10.1016/j.jbiomech.2016.01.002
[11] Buchanan Jr, John R., Clement Kleinstreuer, George A. Truskey, and Ming Lei. "Relation between non-uniform hemodynamics and sites of altered permeability and lesion growth at the rabbit aorto-celiac junction." *Atherosclerosis* 143, no. 1 (1999): 27-40. https://doi.org/10.1016/S0021-9150(98)00264-0
[12] Janela, João, Alexandra Moura, and Adélia Sequeira. "A 3D non-Newtonian fluid–structure interaction model for blood flow in arteries." *Journal of Computational and applied Mathematics* 234, no. 9 (2010): 2783-2791.

https://doi.org/10.1016/j.cam.2010.01.032

[13] Chabannes, Vincent, Gonçalo Pena, and Christophe Prud'Homme. "High-order fluid–structure interaction in 2D and 3D application to blood flow in arteries." *Journal of Computational and Applied Mathematics* 246 (2013): 1-9. https://doi.org/10.1016/j.cam.2012.10.006

[14] Ojha, Matadial, Richard SC Cobbold, K. Wayne Johnston, and Richard L. Hummel. "Pulsatile flow through constricted tubes: an experimental investigation using photochromic tracer methods." *Journal of fluid mechanics* 203 (1989): 173-197. https://doi.org/10.1017/S0022112089001424

[15] Türk, Önder, Münevver Tezer-Sezgin, and Canan Bozkaya. "Finite element study of biomagnetic fluid flow in a symmetrically stenosed channel." *Journal of Computational and Applied Mathematics* 259 (2014): 760-770. https://doi.org/10.1016/j.cam.2013.06.037

[16] Mittal, R., S. P. Simmons, and H. S. Udaykumar. "Application of large-eddy simulation to the study of pulsatile flow in a modeled arterial stenosis." *J. Biomech. Eng.* 123, no. 4 (2001): 325-332. https://doi.org/10.1115/1.1385840

[17] Razavi, Modarres, M. R. SH Seyedein, P. B. Shahabi, and S. H. Seyedein. "Numerical study of hemodynamic wall parameters on pulsatile flow through arterial stenosis." *International Journal of Industrial Engineering & Production Research* 17, no. 3 (2006): 37-46.

[18] Ikbal, Md A., S. Chakravarty, Kelvin KL Wong, J. Mazumdar, and Prashanta K. Mandal. "Unsteady response of non-Newtonian blood flow through a stenosed artery in magnetic field." *Journal of Computational and Applied Mathematics* 230, no. 1 (2009): 243-259. https://doi.org/10.1016/j.cam.2008.11.010

[19] Toufique, Hasan ABM, and Dipak Kanti Das. "Numerical simulation of sinusoidal fluctuated pulsatile laminar flow through stenotic artery." (2008): 25-35.

[20] Ali, N., A. Zaman, and M. Sajid. "Unsteady blood flow through a tapered stenotic artery using Sisko model." *Computers & Fluids* 101 (2014): 42-49. https://doi.org/10.1016/j.compfluid.2014.05.030

[21] Ishikawa, Takuji, Shuzo Oshima, and Ryuichiro Yamane. "Vortex enhancement in blood flow through stenosed and locally expanded tubes." *Fluid Dynamics Research* 26, no. 1 (2000): 35. https://doi:10.1016/S0169-5983(98)00047-1

[22] Kumar, BV Rathish, and K. B. Naidu. "Hemodynamics in aneurysm." *Computers and biomedical research* 29, no. 2 (1996): 119-139. https://doi.org/10.1006/cbmr.1996.0011

[23] Miah, Md Abdul Karim, Ifat Rabbil Qudrat Ovi, Nasimul Eshan Chowdhury, Shorab Hossain, Md Nurul Absar Chowdhury. "Computational investigation of pulsatile blood flow through sinusoidal stenoses of varying lengths." *Journal of Engineering and Technology(JET)* 14, no. 1 (2018): 1-6.

[24] Husain, I., C. Langdon, and J. Schwark. "Non-Newtonian pulsatile blood flow in a modeled artery with a stenosis and an aneurysm." *Rec. Res. Envi. Geo. Sc*: 413-418.

[25] Gopalakrishnan, S.S., B. Pier, and A. Biesheuvel. "Dynamics of pulsatile flow through model abdominal aortic aneurysms." *Journal of Fluid Mechanics* 758 2014: 150-179. https://doi.org/10.1017/jfm.2014.535

[26] Haghighi, Ahmad R., and Nikou Pirhadi. "A Numerical Study of Heat Transfer and Flow Characteristics of Pulsatile Blood Flow in a Tapered Artery with a Combination of Stenosis and Aneurysm." *Journal homepage: http://iieta. org/Journals/IJHT* 37, no. 1 (2019): 11-21. https://doi.org/10.18280/ijht.370102

[27] Kono, Kenichi, Osamu Masuo, Naoyuki Nakao, and Hui Meng. "De novo cerebral aneurysm formation associated with proximal stenosis." *Neurosurgery* 73, no. 6 (2013): 1080-1090. https://doi.org/10.1227/NEU.0000000000000065

[28] Sonia, Hammami, Ben Hamda Khaldoun, Mahjoub Sylvia, Maatoug Faouzi, Gamra Habib, and Ben Farhat Mohamed. "Stenosis and aneurysm of coronary arteries in a patient with Behçet's disease." *The open cardiovascular medicine journal* 2 (2008): 118. https://doi.org/10.2174/1874192400802010118

[29] Zaman, Akbar, Nasir Ali, and O. Anwar Bég. "Numerical simulation of unsteady micropolar hemodynamics in a tapered catheterized artery with a combination of stenosis and aneurysm." *Medical & biological engineering & computing* 54, no. 9 (2016): 1423-1436. https://doi.org/10.1007/s11517-015-1415-3

[30] Egelhoff, C. J., R. S. Budwig, D. F. Elger, T. A. Khraishi, and K. H. Johansen. "Model studies of the flow in abdominal aortic aneurysms during resting and exercise conditions." *Journal of biomechanics* 32, no. 12 (1999): 1319-1329.

https://doi.org/10.1016/S0021-9290(99)00134-7
[31] Vijayajothi, Paramasivam, Muthusamy Kanesan, M. Rafiq, and Abdul Kadir. "Computer Simulations of Pulsatile Blood Flow in Fusiform Models of Abdominal Aortic Aneurysms." *CFD Letters* 4, no. 2 (2012): 47-53.
[32] Algabri, Yousif A., Surapong Chatpun, and Ishkrizat Taib. "An Investigation of Pulsatile Blood Flow in An Angulated Neck of Abdominal Aortic Aneurysm Using Computational Fluid Dynamics." *Journal of Advanced Research in Fluid Mechanics and Thermal Sciences* 57, no. 2 (2019): 265-274.